Activity of a β-Nucleating Agent for Isotactic Polypropylene and Its Influence on Polymorphic Transitions

C. Marco,[1] M. A. Gómez,[1] G. Ellis,[1] J. M. Arribas[2]

[1]*Departamento de Física e Ingeniería, Instituto de Ciencia y Tecnología de Polímeros, CSIC, c/ Juan de la Cierva 3, 28006 Madrid, Spain*
[2]*Dirección Corporativa de Servicios Compartidos, Dirección Tecnológica de REPSOL-YPF, c/ Embajadores 183, 28045 Madrid, Spain*

Received 21 June 2001; accepted 29 October 2001

ABSTRACT: The influence of a nonpigmenting β-nucleating additive in the crystallization of isotactic polypropylene (iPP) is investigated by differential scanning calorimetry and X-ray diffraction. It is found that this additive induces the formation of a very high level of the trigonal modification of iPP. The crystallization and melting behavior of the nucleated systems are studied as a function of the cooling and heating rates and the control of the final temperature during the cooling process. The nucleating agent exerts an important effect on the crystallization temperatures and the polymorphic transitions of iPP, delaying the β–α recrystallization process through an increase in the stability of the trigonal crystals. © 2002 Wiley Periodicals, Inc. J Appl Polym Sci 86: 531–539, 2002

Key words: polypropylene; nucleation; crystallization; polymorphism; thermal properties

INTRODUCTION

Isotactic polypropylene (iPP) is a polymorphic material that can crystallize in monoclinic (α), trigonal (β), orthorhombic (γ), and smectic modifications, all with a 3_1 helix (tgtg) conformation but with different orientations and packing of the polymer chains in the crystal lattice.[1–12] Of these polymorphs, the α form is the thermodynamically stable crystalline modification and is predominant under common processing conditions. The β form occurs more rarely because of its lower stability than the α form, although it has a higher growth rate. However, the formation of the β modification can be influenced by specific thermal histories such as high crystallization rates,[4] high crystallization temperatures,[1,2] high temperature gradients,[13] or rapid cooling from the melt to 130–135°C.[5] The β form transforms into the α form when heated or annealed by recrystallization and/or transformation of phases.[14–17] The β form can also be obtained from melts exposed to shear stress,[18–21] but it cannot be obtained in fibers because of transformation into the α phase during the orientation process.[22] Also demonstrated was the formation of the β modification induced by monoclinic nuclei that develop on the surface of bubbles generated by contraction of the melt during the crystallization process.[23]

The crystallization of iPP from the melt can be improved in the crystallization region where heterogeneous nucleation occurs by the addition of foreign nuclei to the polymer melt. Nucleating agents reduce the induction time for crystallization because they provide foreign surfaces or nuclei onto which the crystallization is initiated. The presence of solid particles, liquids, and even gas bubbles can nucleate the α form of iPP.[24–28] A series of substances that can act as nucleating agents for the β form, depending on the concentration and dispersion of the additives and the cooling rates, were also described.[14,29–38] The addition of these additives can reduce the cycle time during melt processing because of the higher crystallization rates and influence their physical and mechanical properties. Further, these additives can influence the polymorphic behavior and substantially modify the balance of the final properties of the polymer. As such, the control of the crystallization conditions under which a specific crystalline modification can be formed is essential to the design of materials based on iPP.

The main objective of this study is the investigation of the nucleating activity of a naphthalene dicarboxamide derivative in the crystallization of the β modi-

Correspondence to: C. Marco (cmarco@ictp.csic.es).
Contract grant sponsor: CICYT; contract grant number: MAT98-0914.
Contract grant sponsor: CAM; contract grant number: 07N/0032/1999.
Contract grant sponsor: EU; contract grant number: IHP-HRRI-CT-1999-00040.

Journal of Applied Polymer Science, Vol. 86, 531–539 (2002)

fication of iPP. The thermal behavior of the nucleated iPP was determined under very different crystallization conditions, and the transformations between α and β polymorphs of iPP were also studied as a function of the thermal history and additive concentration.

EXPERIMENTAL

Materials

The iPP sample that was used was a commercial grade supplied by REPSOL-YPF, and it had a viscosity-average molecular weight of 164,700. The characterization is described elsewhere.[39] The nucleating agent was *N,N′*-dicyclohexyl-2,6-naphthalene dicarboxamide (NJSTAR NU100) supplied by NJC-RIKA. The nucleated systems were prepared by melt blending in a twin-screw extruder with a NJSTAR NU100 concentration between 0.05 and 0.3% by weight, using the conditions previously described.[39]

Physical properties

The thermal stability of all samples was studied by thermogravimetric analysis using a Mettler TA-4000/TG-50 thermobalance in an oxygen atmosphere and at a heating rate of 20°C min^{-1}. The temperature that corresponds to the start of the thermal decomposition (T_i) was obtained from the thermogravimetric curves.

The thermal properties were analyzed under dynamic conditions in a Perkin–Elmer DSC7/7700/UNIX differential scanning calorimetry (DSC) instrument calibrated with indium (melting temperature, T_m, = 156°C; melting enthalpy, ΔH_m, = 28.45 J g^{-1}). The experiments were carried out in a nitrogen atmosphere using 10–12 mg of sample sealed in an aluminum pan. The T_m values were taken as the peak maximums of the endothermic curves. The temperatures that correspond to the initiation of the crystallization (T_{ic}) and the maxim of the exothermic peak (T_c) were chosen as the characteristic temperatures for the dynamic crystallization process. The degree of crystallinity ($1 - \lambda$) was calculated from the ratio $\Delta H_a/\Delta H_u$, where ΔH_a and ΔH_u are the apparent and completely crystalline heats of fusion, respectively. The values of 177.0 and 168.5 J g^{-1} were used for the ΔH_u for 100% crystalline α-iPP and 100% crystalline β-iPP, respectively.[40] Different thermal treatments were investigated by DSC after melting the samples in the calorimeter at 210°C for 10 min: in one treatment they were cooled to 40°C at 1, 2, 5, 10, and 20°C min^{-1} and subsequently heated to 210°C at 10°C min^{-1}; in the other they were cooled to 40°C at 1 and 20°C min^{-1} and subsequently heated to 210°C at 1 or 20°C min^{-1}.

Thermooptical studies were carried out in transmitted visible light by using a Reichert Zetopan Pol polarizing microscope and a Mettler FP-80HT hot stage with a Nikkon FX35A 35-mm SLR camera.

Wide angle X-ray (WAXS) diffractograms of the samples were obtained at room temperature using a Rigaku Geigerflex-D/max X-ray diffractometer (fitted with a RU-200 rotating anode generator) at 1° min^{-1} in a 2θ range between 5 and 35° using Ni-filtered CuKα radiation. Real-time WAXS and small angle X-ray diffraction (SAXS) patterns were simultaneously recorded using synchrotron radiation at the polymer beamline at Hasylab (DESY, Hamburg) with a double focusing camera.[41] The beam was monochromatized (0.15 nm) by Bragg reflection at a germanium single crystal, which was bent in order to focus the beam in the horizontal direction. A mirror was used for focusing in the vertical direction. The WAXS and SAXS scatter was detected using linear Gabriel detectors. Further details regarding the instrumentation are given elsewhere.[42] The scattering intensity was divided by the intensity of the primary beam, which was measured by an ionization chamber in relative units, in order to consider the change of the intensity of the primary beam during the measurements. The background scattering obtained when no samples were present in the beam was subtracted from all measured curves after proper correction with respect to absorption. Lorentz correction of the SAXS data was performed by multiplying the intensity by s^2, where $s = 2\sin\theta/\lambda$, 2θ is the scattering angle, and λ is the wavelength. The long period (L) was obtained from the maximum of the SAXS curve. Samples were prepared as films by compression molding. The following thermal histories were investigated: cooling from 210 to 120 or 40°C at 1 and 20°C min^{-1} or heating the samples crystallized under the former conditions at 1°C min^{-1}.

RESULTS AND DISCUSSION

The thermal stability of all samples in an oxygen atmosphere (i.e., under more drastic conditions than the DSC experiments) was determined to confirm that no thermal degradation took place during the different thermal cycles that were performed. The initial degradation temperatures of 225 and 310°C were obtained for iPP and the nucleating agent NJSTAR NU100, respectively. The degradation of the nucleated iPP/NJSTAR NU100 systems started at temperatures between 222 and 226°C, demonstrating that all the materials decompose at temperatures far above the melting temperature used in this work.

The influence of the melting temperature and residence time in the melt on the crystallization rate of the same iPP material was previously investigated in a study of the efficiency of an α-nucleating agent.[39] From this work a thermal history of melting at 210°C

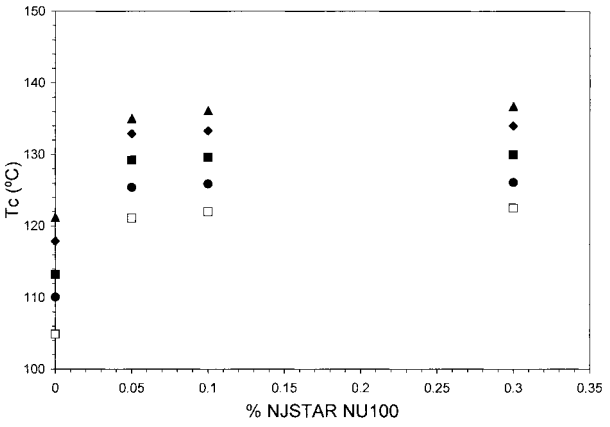

Figure 1 The variation of the crystallization temperatures with the concentration of NJSTAR NU100 at cooling rates of (□) 20, (●) 10, (■) 5, (♦) 2, and (▲) 1 °C min^{-1}.

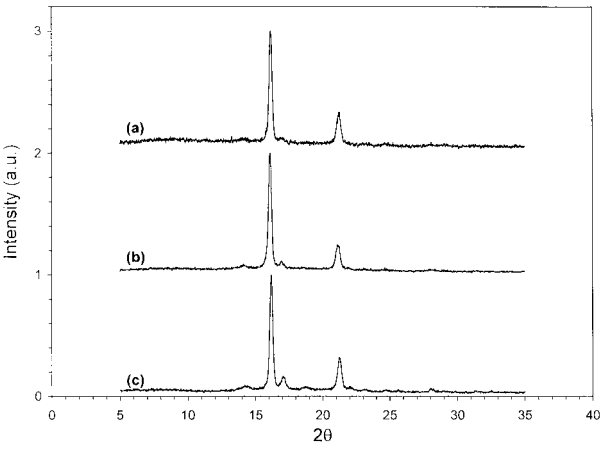

Figure 2 WAXS diffractograms recorded at room temperature for iPP nucleated with 0.05% NJSTAR NU100 and crystallized at cooling rates of (a) 20, (b) 10, and (c) 1 °C min^{-1}.

for 10 min was selected to eliminate melt phase memory effects in the determination of the crystallization rates of the nucleated systems.[43,44]

Figure 1 shows the evolution of the crystallization temperature (T_c) with the concentration of the nucleating agent at different cooling rates. In all cases a single exotherm was observed and a very important increase in the T_c was found for the lowest concentration of the additive, which levels out at the highest concentration of nucleating agent, reaching a maximum increment between 15 and 18°C. The same behavior was observed when the temperature that corresponds to the T_{ic} was monitored, although a slightly lower increment was observed. The T_c values and the corresponding changes in crystallization enthalpy (ΔH_{ci}) are shown in Table I for the five cooling rates used in the study.

The X-ray diffraction patterns of a sample of iPP with 0.05% NJSTAR NU100 were recorded at room temperature after dynamic crystallization at the indicated cooling rates, which are shown in Figure 2. The two main reflections characteristic of the iPP β modification are clearly observed at $2\theta = 16.2$ and 21.2°, which are associated with the (300) and (301) planes, respectively, together with three other reflections of very low intensity at $2\theta = 14.2$, 17, and 18.8°, which correspond to the respective (110), (040), and (130) planes of the α modification. From the X-ray diffraction patterns, the relative proportion of the β form was calculated using the Turner-Jones et al. parameter[4] (k_β) that is given by

$$k_\beta = \{(I_{\beta 1})/[I_{\beta 1} + (I_{\alpha 1} + I_{\alpha 2} + I_{\alpha 3})]\} \qquad (1)$$

where $I_{\beta 1}$ is the intensity of the (300) reflection of the β modification and $I_{\alpha 1}$, $I_{\alpha 2}$, and $I_{\alpha 3}$ are the intensities of the (110), (040), and (130) reflections, respectively, of the α modification. Values of k_β between 0.85 and 0.95 were obtained for all nucleated systems; the higher the cooling rate, the larger the increase in the level of the β form, indicating that increasing the cooling rate considerably reduces the number of monoclinic crystallites formed during the dynamic crystallization process.

The values of the melting temperatures obtained in heating cycles at 10°C min^{-1} subsequent to the dynamic crystallization at different cooling rates are indicated in Table II. Multiple endotherms were observed in all cases, as can be seen in the example in Figure 3. In the absence of different crystalline forms, the observation of multiple endotherms in iPP was assigned to the existence of two different spherulitic

TABLE I
Crystallization Temperatures and Enthalpies for iPP-Nucleated Systems at Different Cooling Rates as Function of Nucleating Agent Composition

Nucleating agent (%)	$T_{c_{20}}$ (°C)	$T_{c_{10}}$ (°C)	T_{c_5} (°C)	T_{c_2} (°C)	T_{c_1} (°C)	$\Delta H_{c_{20}}$ (°C)	$\Delta H_{c_{10}}$ (°C)	ΔH_{c_5} (°C)	ΔH_{c_2} (°C)	ΔH_{c_1} (°C)
0	104.9	110.1	113.2	117.9	121.2	89.3	93.5	94.8	95.5	94.9
0.05	121.1	125.4	129.2	132.9	135.0	85.0	90.1	93.3	95.6	97.4
0.1	122.0	125.9	129.6	133.3	136.1	86.1	90.7	92.9	95.4	96.5
0.3	122.5	126.1	130.0	134.0	136.7	86.4	91.6	94.9	96.8	98.3

TABLE II
Melting Temperatures Subsequent to Dynamic Crystallization at Different Cooling Rates as Function of Nucleating Agent Composition

Nucleating agent (%)	$T_{m_{20}}$ (°C)	$T_{m_{10}}$ (°C)	T_{m_5} (°C)	T_{m_2} (°C)	T_{m_1} (°C)
0	168.7	166.2	164.5	164.5	166.9
0.05	153.7	155.3	156.1	157.5	158.6
	170.4	169.9	169.9	168.2	168.3
0.1	153.7	155.5	156.8	158.1	158.7
	170.4	170.6	169.9	169.6	168.3
0.3	154.7	155.4	156.7	158.4	159.4
	170.4	170.6	169.0	168.8	168.2

structures,[45] different crystal sizes,[46] and recrystallization and reorganization of the imperfect monoclinic crystals during heating.[47] The double melting peak can also be associated with the recrystallization of the monoclinic α_1 phase into the more ordered α_2 phase.[48] In our case, the low temperature endotherm is located between 153 and 159°C and corresponds to the melting of the β crystals. The peak maximum of the endotherm does not change with the content of nucleating agent; but it increases in temperature when the cooling rate of the dynamic crystallization decreases, indicating the formation of more perfect or larger crystals.

The endotherm at high temperature can be associated with the melting of the α crystals, and it is located between 168 and 171°C with a very low enthalpy. The peak maximum is also independent of the nucleating additive concentration, but its relative area diminishes when the cooling rate of the crystallization process is reduced. These results contradict those explained above from the X-ray diffraction experiments, which showed a decrease of the α-crystalline fraction with an increase in the cooling rate during the crystallization

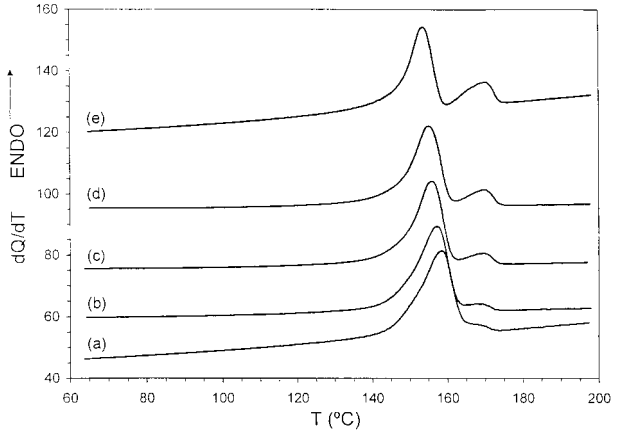

Figure 3 Melting endotherms of iPP with 0.05% NJSTAR NU100 recorded at 10°C min^{-1} after crystallization at cooling rates of (a) 1, (b) 2, (c) 5, (d) 10, and (e) 20°C min^{-1}.

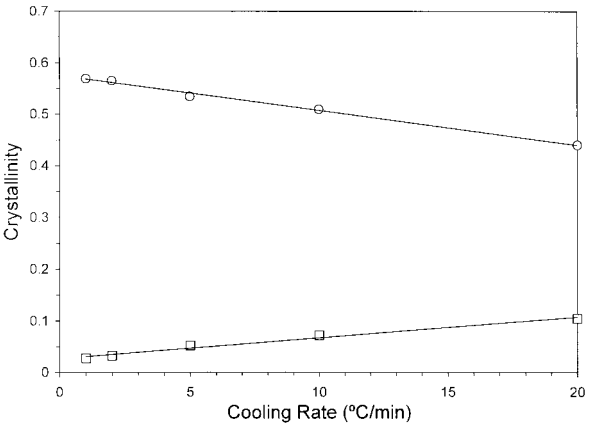

Figure 4 The variation of the crystallinity associated with the (□) α and (○) β form in iPP/NJSTAR NU100 with 0.05% additive concentration, which is obtained from the melting endotherms recorded at 10°C min^{-1} as a function of the cooling rate.

process. Figure 3 clearly shows that the relationship between the areas of the endotherms associated with the melting of trigonal and monoclinic crystals (A_β/A_α) decreases with an increasing cooling rate. The evolution of each independent endotherm with the composition and cooling rate can be obtained by applying a peak deconvolution process to the total DSC endotherm (Table II), although it should be pointed out that the effect of the exothermic β–α recrystallization, which takes place during the heating cycle, on the enthalpy values is very difficult to assess. The degree of crystallinity ($1 - \lambda$) associated with each phase can be obtained from the deconvoluted peaks using the values of ΔH_u, which correspond to the 100% crystalline α- and β-polypropylene, respectively,[40] as described in the Experimental section. The β fraction (X_β) was estimated from DSC by the following expression:

$$X_\beta = (1 - \lambda)_\beta / [(1 - \lambda)_\beta + (1 - \lambda)_\alpha] \qquad (2)$$

Figure 4 shows the variation of ($1 - \lambda$) associated with each phase for an iPP sample nucleated with 0.05% NJSTAR NU100. We observed that as the cooling rate of the crystallization process increases, the degree of crystallinity of the β phase diminishes and the degree of crystallinity of the α phase increases.

Several other conclusions can be reached from the thermograms shown in Figure 3. Splitting of the low temperature endotherm associated with the β crystals is not observed, indicating the absence of a β–β' recrystallization, as could be expected because the samples were cooled to 40°C, which is well below the critical temperature ($T_{\alpha\beta}$) described by Varga et al.[14,15] Further, an exothermic process between both endotherms is not observed, which may indicate the ab-

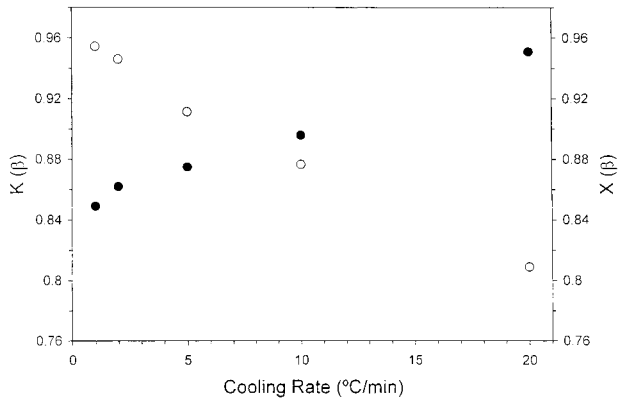

Figure 5 A comparison of k_β values obtained from the WAXS diffractograms at (●) room temperature and the fraction of the β form obtained from the melting endotherm heating at (○) 10°C min^{-1} for iPP/NJSTAR NU100 with 0.05% additive concentration.

sence of β–α recrystallization, which usually takes place when the samples are cooled below $T_{\alpha\beta}$.[14,15] However, the comparison between the fraction of β crystals obtained from the DSC data and the amount of the β phase in the material calculated from the X-ray diffractograms (Fig. 5) demonstrates the existence of a β–α transition that considerably increases the fraction of monoclinic crystals that melt, increasing the area of the high temperature endotherm. The more imperfect the trigonal crystals are (i.e., at higher cooling rates), the more important the β–α transition becomes.

Several crystallization and melting cycles were performed at different rates to clarify the melting behavior of the iPP nucleated systems with NJSTAR NU100. As an example of the behavior observed in all nucleated systems, Figure 6 shows the melting thermograms for iPP with 0.05% nucleating agent. When the sample is cooled from the melt to 40°C at 20°C min^{-1} and subsequently heated at 1°C min^{-1}, an exothermic β–α transition is observed immediately after the low temperature endotherm located at 152°C [Fig. 6(a)]. It was stated[14,15] that β-iPP samples are susceptible to β–α recrystallization before melting if they are cooled below $T_{\alpha\beta}$, which is induced by the α phase formed during secondary crystallization at temperatures below $T_{\alpha\beta}$.[1,13,30,49–51] Further, if we compare the ratio of peak areas A_β/A_α obtained in Figure 6(a) to that in Figure 3, the relation is inverted, showing an increase in the fraction of monoclinic crystals in the transition. The same behavior is observed when the sample is cooled to 40°C at 1°C min^{-1} and subsequently heated at 1°C min^{-1} [Fig. 6(b)]. However, in this case the area associated with the monoclinic phase does not display such a spectacular increase with respect to the trigonal phase, which indicates lower nucleating activity of these crystals; rather, it shows a splitting of the endotherm associated with the α_1 and α_2 phases at 167 and 169°C, respectively. The new monoclinic crystals that form during the β–α transition are α_2 and melt at a higher temperature than the α_1 monoclinic crystals formed during cooling from the melt. The tendency for β–α recrystallization in iPP was attributed to the formation of monoclinic crystals within the β spherulites because of secondary crystallization in the cooling process below $T_{\alpha\beta}$. These finely distributed monoclinic crystals act as α-nucleating agents during the partial melting of the β phase and generate the monoclinic α_2 phase.[7,14,38]

The morphology of the iPP/NJSTAR NU100 samples developed during these thermal cycles was analyzed by polarized optical microscopy. Figure 7(a) shows the presence of two types of spherulites formed on cooling to 40°C at 1°C min^{-1}. Highly birefringent, type III spherulites characteristic of the β phase are observed, together with mixed radial spherulites associated with the α phase. On heating at temperatures between 145 and 154°C, these type III spherulites adopt a different spherulitic structure with a lower birefringence and are dissimilar from the mixed radial α spherulites [Fig. 7(b–d)]. These new spherulites are stable at 160°C and melt at 170°C [Fig. 7(e)].

The crystallization and melting processes of the nucleating systems were also investigated by real-time WAXS and SAXS experiments using synchrotron radiation. In Figure 8 the WAXS diffractograms recorded during the cooling process at 1°C min^{-1} are shown for iPP with 0.05% nucleating agent. The formation of the (300) and (301) reflections associated with the β phase are clearly observed at 134°C and completely developed at 120°C, together with the very low intensity (110) reflection corresponding to the α phase that appears at 134°C. When heated, the growth

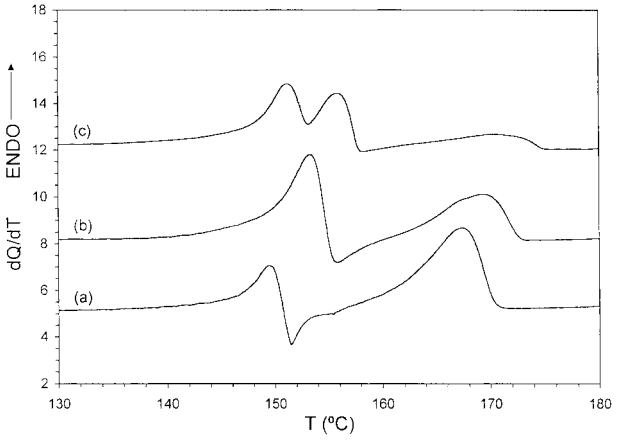

Figure 6 Melting endotherms of iPP/NJSTAR NU100 with 0.05% additive concentration recorded at 1°C min^{-1} after dynamic crystallization under the following conditions: cooling to 40°C at (a) 20 and (b) 1°C min^{-1} and (c) cooling to 120°C at 20°C min^{-1}.

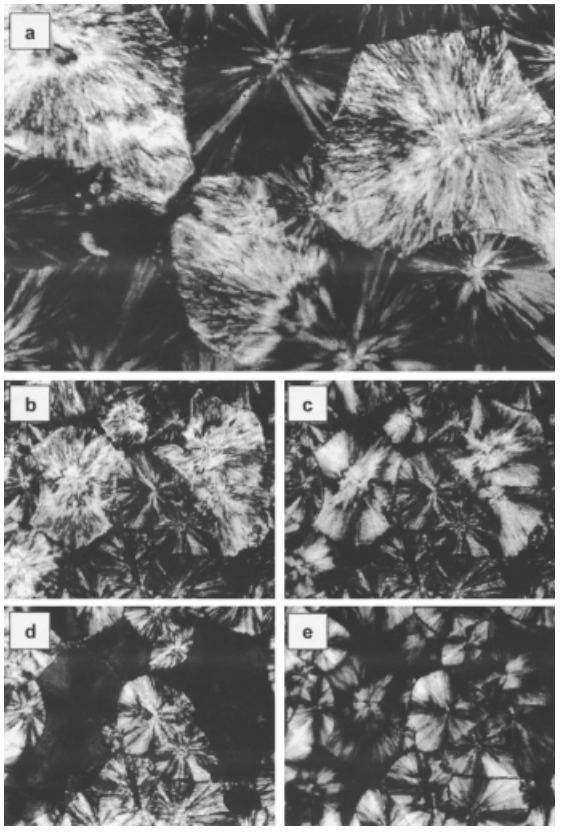

Figure 7 Optical micrographs of iPP/NJSTAR NU100 with 0.05% additive concentration under the following conditions: (a) at 40°C after crystallization when cooling from 210°C at 1°C min^{-1} and when heating the sample at 1°C min^{-1} to (b) 145, (c) 150, (d) 154, and (e) 160°C.

of the (110), (040), (130), and (301) reflections of the α phase are observed at 150°C, as is a reduction in the intensity of those associated with the β phase, which completely disappears at 156°C (Fig. 9). The Lorentz corrected SAXS data recorded simultaneously during the same heating cycle show changes in the intensity and position of the peak maxims. The intensity of the SAXS peak decreases on heating, reaching a minimum at 152°C, followed by a slight increase and leveling out at 157–159°C and a subsequent decrease up to 170°C. This behavior is presented in Figure 10, along with that corresponding to the variation with temperature of the L associated with the maximum of the SAXS peak. The increase observed in L values between 130 and 140°C can be explained by the melting of the small and imperfect β crystals generated during crystallization from the melt. At 145°C an important increase in L and a decrease in intensity are observed that corresponds to the melting of the more perfect and bigger β-form crystals. From 150 to 155°C the decrease observed in the L values and the changes at the same temperature in the WAXS patterns shown in Figure 9 can be associated with the formation of monoclinic crystals by recrystallization from β structures, and these demonstrate the existence of a β–α transformation.

Figure 11 compares the variation with temperature of the k_β obtained from the WAXS data with the evolution of the total area of the SAXS peak. Up to 142°C the fraction of β crystals remains constant while the total area falls slightly, and this can be related to the melting of small β crystals. From 142 to 153°C an accelerated decrease in the k parameter is observed that is due to complete melting of all the β crystals. The area decreases up to 152°C, but from this temperature to around 156°C an increase is observed that correlates with the formation of α crystals.

The diffraction results and those obtained by DSC and optical microscopy demonstrate that in our nucleated systems monoclinic crystals form from the melting process of the trigonal crystals generated during crystallization, which is in agreement with similar observations for other β-nucleating agents.[52,53]

A number of different interpretations for the mechanism of the β–α transformation were suggested. Samuels and Yee[54] proposed the formation of a liquid phase because of the considerable differences in the unit cell of the two structures; Asano and Fujiwara[55] suggested that this transformation occurs by unfold-

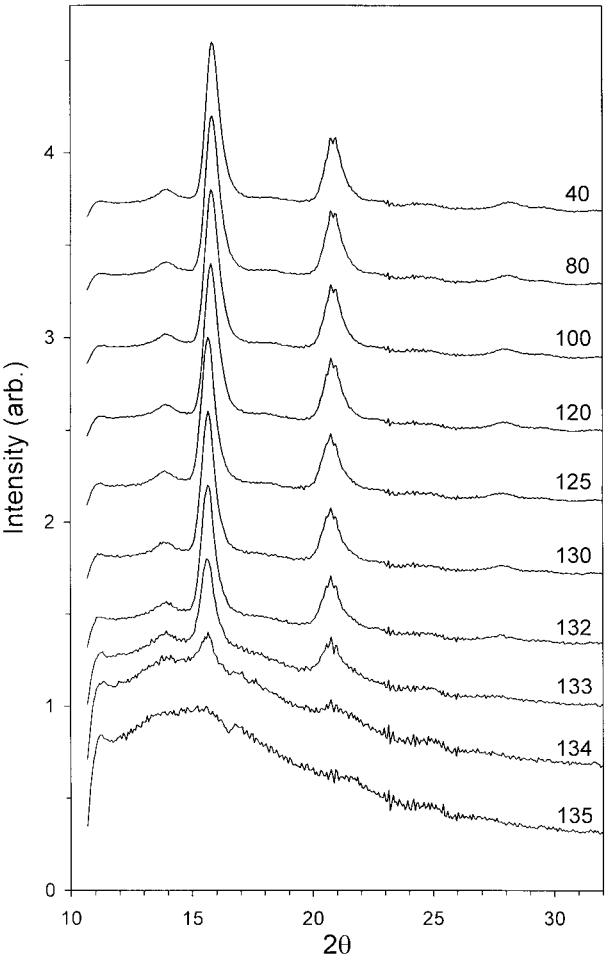

Figure 8 WAXS diffractograms of iPP nucleated with 0.05% NJSTAR NU100 when cooling from 210 to 40°C at 1°C min^{-1}.

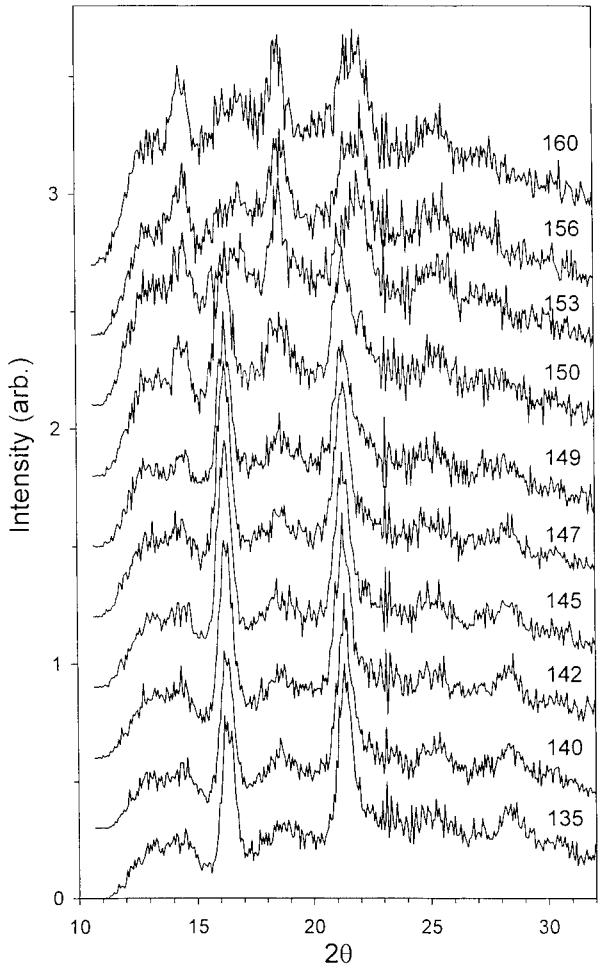

Figure 9 WAXS diffractograms of iPP nucleated with 0.05% NJSTAR NU100 when heating at 1°C min^{-1} after the crystallization cycle shown in Figure 8

ing, melting, and recrystallization; and Garbarczyk et al.[53] suggested that β–α recrystallization is preceded by the transition of the β phase into a disordered state. The β–α transformation does not take place automatically with the disappearance of the β form; it occurs

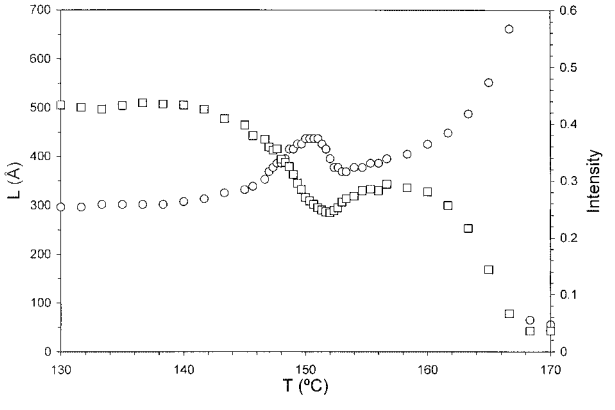

Figure 10 The variation of (○) L and the intensity of the (□) SAXS peak for iPP nucleated with 0.05% NJSTAR NU100 when heating at 1°C min^{-1} after dynamic crystallization by cooling from 210 to 40°C at 1°C min^{-1}.

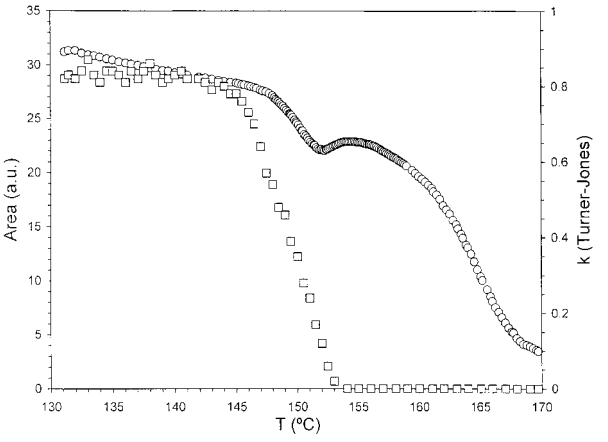

Figure 11 The total area obtained from the (○) SAXS peak and the variation of (□) k_β obtained from the WAXS diffractograms of iPP nucleated with 0.05% NJSTAR NU100 when heating at 1°C min^{-1} after dynamic crystallization by cooling from 210 to 40°C at 1°C min^{-1}.

only when the necessary energy to overcome the energy barrier of the transformation is reached.[56] Extensive DSC studies by Varga et al.[14,15] demonstrated partial melting of the β form during the heating cycle after cooling below 100°C, results that were confirmed by Fillon et al.[17] by DSC and optical microscopy measurements.

The influence of the final temperature that was selected on cooling from the melt was analyzed in our nucleated iPP systems by cooling the samples to 120°C at 20°C min^{-1}, a temperature above the critical temperature $T_{\alpha\beta}$. The subsequent heating cycle at 1°C min^{-1} is shown in Figure 6(c) for the system with 0.05% NJSTAR NU100 as an example. A splitting of the melting peak of the β phase can be clearly observed and is related to a β–β′ transition, and an important decrease in the endotherm associated with the monoclinic phase is also found. The β–β′ transition is related to a stabilization or perfection of the structure of the β modification without a transition between different crystalline forms, as can be confirmed in the X-ray data presented in Figure 12. The existence of the β–β′ transformation indicates structural instability of the β phase, favored in this case by a very low heating rate.[14,15]

One of the more effective families of β-nucleating agents are pimelic acid/calcium stearate blends, which give k_β values of between 0.6 and 0.94, depending on the relative concentration of both components and the total concentration and degree of dispersion of the nucleating agents.[36,37,57,58] Calcium suberate was also recently shown to be an effective and selective β-nucleation agent.[59] Another typical nucleating agent that efficiently induces the crystallization of iPP in the β modification is quinacridone (commercially known as E3P),[60] which generates k_β values of 0.6–0.7 for iPP systems prepared by roll mixing or 0.28–0.54 for samples prepared by extrusion.[31] It was recently deter-

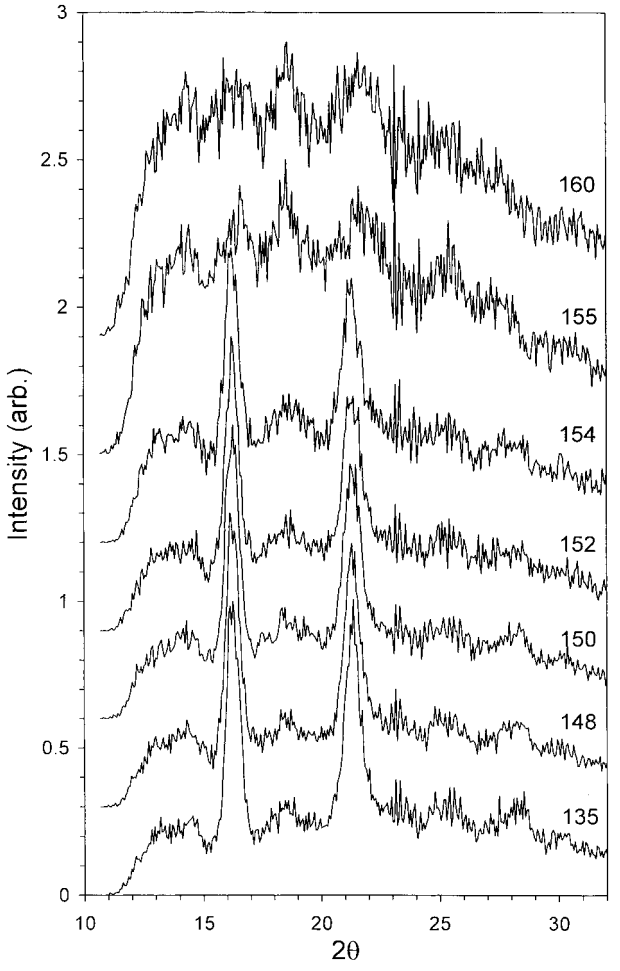

Figure 12 WAXS diffractograms of iPP nucleated with 0.05% NJSTAR NU100 when heating at 1°C min^{-1} after dynamic crystallization by cooling from 210 to 120°C at 20°C min^{-1}.

mined that the use of pigments in polypropylene fibers give β-form contents that are dependent on the spinning velocity, reducing k_β to 0.11–0.4, for example, when the fibers are spun at high velocity.[61] However, k_β values of 0.9 were obtained with other pigments,[62] and the important influence of the nucleating agent concentration was demonstrated.[63] Garbarczyk and Paukszta[29,64] studied the influence of a series of additives (based on aromatic amines and their sulfur derivatives) on the formation of the β modification of iPP. They determined k_β values between 0.07 and 0.67 for mercaptobenzimidazole, phenothiazine, and triphenodithiazin and k_β values between 0.25 and 0.30 for anthracene and phenanthrene. They concluded that the β form occurs only when the structure of the additives is quasiplanar, suggesting the formation of complexes of the additive and the polymer. They also established that the β–α transformation is retarded or eliminated, depending on different physicochemical factors related to the β-nucleating agent.[29] They found that those additives with high k_β values showed a greater influence on the retardation phenomena. A retardation

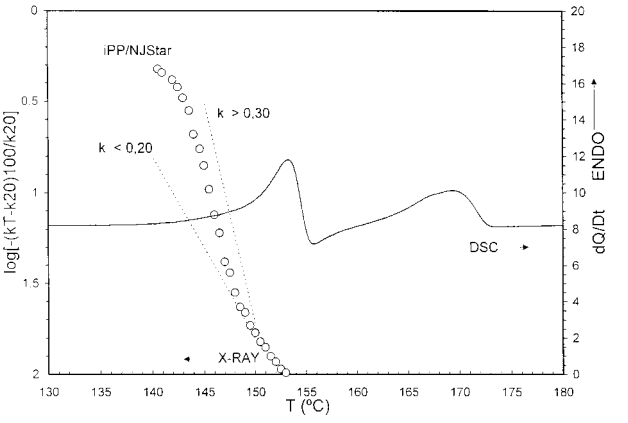

Figure 13 A comparison of the retardation factor for iPP nucleated with 0.05% NJSTAR NU100 heated at 1°C min^{-1} after dynamic crystallization when cooling from 210 to 40°C at 1°C min^{-1} versus the additives described in Beck.[26]

factor can be obtained from the slope of $\log(-\Delta k \times 10^2/k_{20})$ versus temperature, where Δk is the difference between k at a given temperature and k at 20°C.

Figure 13 compares the results obtained for iPP nucleated with NJSTAR NU100 with the results of the behavior of other nucleating agents from the literature.[29] Observe that the data obtained from the X-ray measurements are in perfect agreement with those obtained from DSC in the same crystallization conditions, assuming that the β–α transition takes place at a higher temperature and the faster the rate is the higher the fraction of β crystals in the material, as was described for some nucleating agents with similar structure and k_β values higher than 0.3.[29]

In a study of organic pigments with β-nucleating activity, which all have fused benzene rings or heterocycles in their molecular structure, a wide range of k_β values was observed (Table III). It was shown that a common feature in the diffraction patterns was that the strongest or second strongest reflection was located at a d-spacing of 0.283 nm,[65] a value that is about half that of the β form (300), which is 0.564 nm. In later studies of the nucleation of iPP with γ-quinacridone, triphenodithiazin, and dicyclohexylterephthalamide, it was established that the nucleating agents with a periodicity of 0.65 nm and an orthogonal geometry on the contact face can induce a β modification.[34,66] When

TABLE III
Values of k_β Observed for Concentration of 0.05% of Range of Organic Pigments

Pigment name	k_β
Indigosol Brown IRRD	0.54
Indigosol Red Violet IRH	0.68
Cibantine Orange HR	0.82
Indigosol Pink IR	0.82
Cibantine Blue 2B	0.86
Indigosol Golden Yellow IGK	0.92
Indigosol Grey IBL	0.95

the X-ray diffractograms of the nucleating agent NJSTAR NU100 and other iPP nucleated samples are compared, it should be pointed out that none of the above characteristics for other β-nucleating agents exist in this additive, and only an overlap between the reflections at $2\theta = 21°$ with a d-spacing of 0.42 nm is observed.

CONCLUSIONS

The investigation of a nonpigmenting nucleating agent found it to be very efficient at inducing the crystallization of iPP into the β modification with k_β values between 0.85 and 0.95, depending on the concentration of the additive and the cooling rate. The crystallization temperatures of the nucleated system are strongly affected, showing an important increase even for the lowest concentration of the additive. The melting behavior of the nucleated iPP was also analyzed, and the influence of the additive on the existence and nature of the β–α transformation was established. In the presence of NJSTAR NU100 the β–α transition is retarded with respect to other additives, taking place at higher temperature and over a very small temperature interval.

The authors wish to thank C. Blancas (REPSOL-YPF), M. A. López Galán (ICTP), and M. Garcia (ICTP) for their collaboration. The financial support from the CICYT and CAM is gratefully acknowledged. The work at the DESY Synchroton facility in Germany was supported by the European Commission IHP Programme.

References

1. Padden, F. J.; Keith, H. D. J Appl Phys 1959, 30, 1479.
2. Keith, H. D.; Padden, F. J.; Walter, N. M.; Wyckokk, H. W. J Appl Phys 1959, 30, 1485.
3. Natta, G.; Corradini, P. Nuovo Cimento 1960, 15, 40.
4. Turner-Jones, A.; Aizlewood, J. M.; Beckett, D. R. Makromol Chem 1964, 75, 134.
5. Norton, D. R.; Keller, A. Polymer 1985, 26, 704.
6. Meille, S. V.; Brückner, S.; Porzio, W. Macromolecules 1990, 23, 4114.
7. Varga, J. J Mater Sci 1992, 27, 2557.
8. Meille, S. V.; Ferro, D. R.; Brückner, S.; Lovinger, A. J.; Padden, F. J. Macromolecules 1994, 27, 2615.
9. Lotz, B.; Kopp, S.; Dorset, D. C. R. Acad Sci (Paris) 1994, 319, 187.
10. Turner-Jones, A.; Cobbold, A. J. Polym Lett 1968, 6, 539.
11. Ferro, D. R.; Meille, S. V.; Brückner, S. Macromolecules 1998, 31, 6926.
12. Lotz, B.; Wittmann, J. C.; Lovinger, A. J. Polymer 1996, 37, 4979.
13. Lovinger, A. J.; Chua, J. O.; Gryte, C. C. J Polym Sci Polym Phys Ed 1977, 15, 641.
14. Varga, J. J Therm Anal 1986, 31, 165.
15. Varga, J.; Gabor, G.; Ille, A. Angew Makromol Chem 1986, 142, 171.
16. Passingham, C.; Hendra, C. P. J.; Cudby, M. E. A.; Zichy, V.; Weller, M. Eur Polym J 1990, 26, 631.
17. Fillon, B.; Thierry, A.; Wittmann, J. C.; Lotz, B. J Polym Sci Polym Phys Ed 1993, 31, 1407.
18. Devaux, E.; Chabert, B. Polym Commun 1991, 32, 464.
19. Zipper, P.; Janosi, A.; Wrentschur, E.; Abuja, P. M.; Knabl, C. Prog Colloid Polym Sci 1993, 93, 377.
20. Leugering, H. J.; Kirsch, G. Agnew Makromol Chem 1973, 33, 17.
21. Varga, J.; Karger-Kocsis, J. J Polym Sci Part B Polym Phys Ed 1996, 34, 657.
22. Riekel, C.; Karger-Kocsis, J. Polym Commun 1999, 40, 541.
23. Varga, J.; Ehrenstein, G. W. Polymer 1996, 37, 5959.
24. Wunderlich, B. Macromolecular Physics, Volume 2: Crystal Nucleation, Growth, Annealing; Academic: New York, 1976; p 44.
25. Binsbergen, F. L.; de Lange, B. G. M. Polymer 1970, 11, 309.
26. Beck, H. N. J Appl Polym Sci 1967, 11, 673.
27. Menczel, J.; Varga, J. J Therm Anal 1983, 28, 161.
28. Kowalewski, T.; Galeski, A. J Appl Polym Sci 1989, 32, 2919.
29. Garbarczyk, J.; Paukszta, D. Colloid Polym Sci 1985, 263, 985.
30. Shi, G. Y.; Zhang, X. D.; Qiu, Z. X. Makromol Chem 1992, 193, 583.
31. Jacoby, P.; Bersted, B. H.; Kissel, W. J.; Smith, C. E. J Polym Sci Polym Phys Ed 1986, 24, 461.
32. Liu, J.; Wei, X.; Guo, Q. J Appl Polym Sci 1990, 4, 2829.
33. McGenity, P. M.; Hooper, J. J.; Payntes, C. D.; Rilley, A. M.; Nutbeem, C. K.; Elton, N. J.; Adams, J. M. Polymer 1992, 33 5215.
34. Stocker, W.; Schumacher, M.; Graff, S.; Thierry, A.; Wittmann, J. C.; Lotz, B. Macromolecules 1998, 31, 807.
35. Bauer, T.; Thomann, R.; Mülhaupt, R. Macromolecules 1998, 31, 7651.
36. Shi, G.; Zhang, J. Thermochim Acta 1992, 205, 235.
37. Shi, G.; Zhang, J.; Cao, Y.; Hong, J. J Makromol Chem 1993, 194, 269.
38. Varga, J. J Therm Anal 1989, 35, 189.
39. Marco, C.; Gómez, M. A.; Ellis, G.; Arribas, J. M. J Appl Polym Sci 2002, 84, 1669.
40. Li, J. X.; Cheung, W. L.; Demin, J. Polymer 1999, 40, 1219.
41. Hendrix, J.; Koch, M. H. J.; Bordás, J. J Appl Crystallogr 1979, 12, 467.
42. Elsmer, G.; Riekel, C.; Zachmann, H. G. Adv Polym Sci 1985, 1, 67.
43. Ziabicki, A.; Alfonso, G. C. Colloid Polym Sci 1994, 272, 1027.
44. Alfonso, G. C.; Ziabicki, A. Colloid Polym Sci 1995, 273, 317.
45. Aboulfaraj, M.; Ulrich, B.; Danoun, A.; G'Sell, C. Polymer 1993, 34, 4817.
46. Samuels, R. J. J Appl Polym Sci 1975, 13, 1417.
47. Yadav, Y. S.; Jain, D. C. Polymer 1986, 27, 721.
48. Petraccone, V.; Guerra, G.; De Rosa, C.; Tuzi, A. Macromolecules 1985, 18, 813.
49. Rybnikar, F. J Macromol Sci Phys 1991, B30, 201.
50. Karger-Kocsis, J.; Varga, J. J Appl Polym Sci 1996, 62, 291.
51. Karger-Kocsis, J.; Shang, P. P. J Therm Anal 1998, 51, 237.
52. Forgács, P.; Tolochko, B. P.; Sheromov, M. A. Polym Bull 1981, 6, 127.
53. Garbarczyk, J.; Sterzynski, T.; Paukszta, D. Polym Commun 1989, 30, 153.
54. Samuels, R. J.; Yee, R. Y. J Polym Sci Polym Phys Ed 1972, 10, 385.
55. Asano, T.; Fujiwara, Y. Polymer 1978, 19, 99.
56. Garbarczyk, J. J Makromol Chem 1985, 186, 145.
57. Li, J. X.; Cheung, W. L. J Vinyl Add Technol 1997, 3, 151.
58. Li, J. X.; Cheung, W. L. Polymer 1999, 40, 2085.
59. Varga, J.; Mudra, I.; Ehrenstein, G. W. J Appl Polym Sci 1999, 74, 2357.
60. Leugering, H. J. Makromol Chem 1967, 109, 204.
61. Broda, J.; Wlochowicz, A. Eur Polym J 2000, 36, 1283.
62. Radhakrishnan, S.; Tapale, M.; Shah, N.; Rairkar, E.; Shirodkar, V.; Natu, H. P. J Appl Polym Sci 1997, 64, 1247.
63. Seterzynski, T.; Calo, P.; Lambla, M.; Thomas, M. Polym Eng Sci 1997, 37, 191.
64. Garbarczyk, J.; Paukszta, D. Polym Rep 1981, 22, 562.
65. Huang, M. R.; Li, X. G.; Fang, B. R. J Appl Polym Sci 1995, 56, 1323.
66. Lotz, B. Polymer 1998, 39, 4561.